

Magnetoresistance in quasi-one-dimensional metals due to Fermi surface cold spots

Perez Moses and Ross H. McKenzie*

School of Physics, University of New South Wales, Sydney 2052, Australia

(November 20, 2018)

In a number of quasi-one-dimensional organic metals the dependence of the magnetoresistance on the direction of the magnetic field is quite different from the predictions of Boltzmann transport theory for a Fermi liquid with a scattering rate that is independent of momentum. We consider a model in which there are large variations in the scattering rate over the Fermi surface. The model is the quasi-one-dimensional version of the “cold spots” model introduced by Ioffe and Millis to explain anomalous transport properties of the metallic phase of the cuprate superconductors. The dependence of the resistance, in the most and least conducting directions, on the direction and magnitude of the magnetic field are calculated. The calculated magnetoresistance has a number of properties that are quite distinct from conventional transport theory such as magic angle effects and a significant magnetoresistance when the field and current are both in the least conducting direction. However, the model cannot give a complete description of the unusual properties of $(\text{TMTSF})_2\text{PF}_6$ at pressures of 8-11 kbar.

I. INTRODUCTION

Many of the electronic transport properties of strongly correlated metals such as cuprate superconductors,^{1,2} heavy fermions,³ and organic superconductors⁴⁻⁶ are significantly different from elemental metals. The transport properties of the latter are adequately described by Boltzmann transport theory, which is based on a Fermi liquid picture, in which there is one-to-one correspondence between the elementary excitations and those of a non-interacting Fermi gas.⁷ An important and controversial question is whether to describe strongly correlated metals one must completely abandon Fermi liquid theory or whether one can just make modest modifications to Fermi liquid theory, such as allowing the scattering rate to vary significantly over different parts of the Fermi surface. An example of the former point of view for the cuprates is that of Anderson¹ and of the latter is that of Pines⁸ or Ioffe and Millis.⁹ For heavy fermions near a quantum critical point,¹⁰ the former point of view has been advocated by Coleman¹¹ and Smith and Si,¹² and the latter by Rosch.¹³ The only way to resolve this issue is to perform calculations for specific models in order to produce predictions that can be used to falsify that model.

The theoretical description of the magnetoresistance of the metallic phase of the Bechgaard salts, $(\text{TMTSF})_2\text{X}$ [where TMTSF is the tetramethyl-tetraselenafulvene molecule and X is an anion] represents a considerable challenge. The experimental data is briefly summarised below. Strong, Clarke, and Anderson¹⁴ and Zheleznyak and Yakovenko¹⁵ have argued that the data imply a non-Fermi liquid description whereas many others¹⁶⁻²⁰ have tried to explain the data within a Fermi liquid description. None of these theories gives a complete description of the experimental data. The purpose of this paper is to calculate the properties of the magnetoresistance within a “cold spots” model (where the scattering rate varies over the Fermi surface). This model is the quasi-one-dimensional version of a model originally proposed for the cuprates by Ioffe and Millis.⁹ The model has the distinct advantage that it is analytically tractable, allowing the calculation of a wide range of properties of the magnetoresistance that can be compared to experimental results.

We now briefly summarise the observed properties of the magnetoresistance of $(\text{TMTSF})_2\text{X}$ that cannot be explained with Boltzmann transport theory with a simple dispersion relation and a scattering rate that is constant over the Fermi surface. The most puzzling data is that of $(\text{TMTSF})_2\text{PF}_6$ at pressures of about 10 kbar.²¹ We also note that the magnetoresistance of the quasi-two-dimensional metal $\alpha\text{-(BEDT-TTF)}_2\text{MHg(SCN)}_4$ [$\text{M} = \text{K, Rb, Tl}$] also exhibits unusual temperature and angular dependence.^{22,23}

1. *The magic angle effect.* When the magnetic field is rotated in the plane perpendicular to the most conducting direction (i.e., in the $b-c$ plane) one observes dips in the resistance versus angle curve at angles, (where θ is the angle between the field direction and the c -axis) such that $\tan \theta = nb/c$ where b and c are lattice constants and $n = 1, 2, \dots$. The features at $n = 1$ and 2 are most prominent.

2. *Angular dependence.* The simplest Boltzmann transport models predict no magnetoresistance when the magnetic field and current are parallel and the magnetoresistance is a maximum when the field and current are perpendicular. This is observed in $(\text{TMTSF})_2\text{ClO}_4$ at ambient and 6 kbar pressure^{24,25}. However, the opposite is observed in $(\text{TMTSF})_2\text{PF}_6$ at 10 kbar: the magnetoresistance is much larger when the field and current are parallel than when they are perpendicular.²⁴ Specifically, the background magnetoresistance (i.e., after the magic angle effect is subtracted out) only depends on the component of the field perpendicular to the layers. Furthermore, for moderate fields the

resistivity in the most conducting direction, $\rho_{xx} \sim (B \cos \theta)^{0.5}$ and the resistivity in the least conducting direction $\rho_{zz} \sim (B \cos \theta)^{1.3}$. Simple Fermi liquid theory would generally not produce such a non-integer exponent. Note, that this means that there is no magnetoresistance for fields parallel to the b-axis.

3. *Kohler's rule.* In a conventional metal with a single scattering rate this provides a simple way to relate the field and temperature dependence of the resistance. In $(\text{TMTSF})_2\text{ClO}_4$ at ambient pressure²⁶ and at 6kbar²⁵ this is satisfied. However, in $(\text{TMTSF})_2\text{PF}_6$ at 10 kbar there are large violations.

In order to explain the magic angle effect Chaikin first proposed a “hot spots” model, where the scattering rate is significantly larger than elsewhere on the Fermi surface.²⁰ Zheleznyak and Yakovenko did find that the scattering rate due to electron-electron scattering exhibited hot spots. However, these were not of sufficient strength to produce a large magnetoresistance or the magic angle effect.²⁷

In order to explain the anomalous transport properties of cuprates several authors have considered the effects of both hot spots^{28–30} and cold spots^{9,31,32}. Ioffe and Millis⁹ considered a cold spot model where the scattering rate variation had the same symmetry (d-wave) as the superconducting order parameter, i.e., the cold spots are associated with nodes in the energy gap (or pseudogap) which exists in the superconducting phase. Although it is not clear what specific microscopic mechanism produces the cold spots, Ioffe and Millis suggest that they might arise from strong superconducting pairing fluctuations. The model provides a simple explanation of photoemission experiments which show that in the cuprates the electron spectral function varies significantly over the Fermi surface. Along the zone diagonals the spectral function has a well defined quasi-particle peak, suggesting weak scattering; in other regions the spectral function is broad, suggesting strong scattering. Using this simple model and a Boltzmann equation analysis, Ioffe and Millis reproduced quantitatively the frequency and temperature dependence of the observed dc and ac, longitudinal, and Hall conductivities in the cuprates. However, the calculated magnetoresistance is much larger in magnitude and has a stronger temperature dependence than is observed.

In this paper we investigate to what extent such a cold spot model can explain the anomalous magnetoresistance in the quasi-one-dimensional metals, $(\text{TMTSF})_2\text{X}$. We find that the calculated magnetoresistance does have a number of unusual features that are consistent with experiment. (i) When the magnetic field and current are parallel to the least-conducting direction, there is a large positive magnetoresistance. This increases with the strength of the cold spots. (ii) When the magnetic field is rotated in the $b - c$ plane the resistivity in the most-conducting direction has an angular dependence qualitatively similar to the background magnetoresistance of $(\text{TMTSF})_2\text{PF}_6$ at 10 kbar. The resistance is largest when the field is in the least-conducting direction. Furthermore, it only depends on the component of the field parallel to the least conducting direction. (iii) Magic angle effects do occur in the interlayer resistance.

However, there are a number of properties that are inconsistent with experiment. (a) The magnetoresistance saturates with increasing field when the magnetic field and current are parallel to the least-conducting direction. (b) No magic angle effects occur in the resistivity in the most-conducting direction. (c) For reasonable strengths of the magnetic field the size of the features in the interlayer resistance at the magic angles are much smaller than is observed. Further, peaks rather than dips are predicted at the odd-integer magic angles. (d) When the magnetic field is parallel to the b-axis the interlayer magnetoresistance increases quadratically with field, whereas in $(\text{TMTSF})_2\text{PF}_6$ at 10 kbar, it saturates with increasing field. Table I gives a brief summary of the successes and failures of the cold spot model.

The outline of the paper is as follows. In Section II the Boltzmann equation is solved in the relaxation time approximation for the general case of a scattering rate that varies over the Fermi surface. We introduce the specific model for the momentum dependence of the scattering rate that we use. It is shown that in zero field the resistivity is proportional to the inverse of the average of the scattering time over the Fermi surface. In the high field limit the resistivity is proportional to the average of the scattering rate over the Fermi surface. We then show by the use of the Cauchy-Schwarz inequality that the resistance at high fields will always be larger than the resistance at zero field. In Section III the interlayer conductivity in zero field is explicitly evaluated and we consider different models for its temperature dependence. In Section IV the interlayer conductivity is calculated for various directions of the magnetic field. Section V contains a similar calculation for the conductivity in the most conducting direction.

II. BOLTZMANN TRANSPORT THEORY WITH A MOMENTUM-DEPENDENT SCATTERING RATE

A. Derivation of the conductivity

If the scattering rate does not vary over the Fermi surface then the Boltzmann equation can be solved in the relaxation time approximation to yield Chamber's formula for the conductivity in the presence of a magnetic field.⁷ We now consider how this is modified in the presence of a scattering rate that varies over the Fermi surface. Following Ashcroft and Mermin (p.246ff)⁷, let $g(\vec{r}, \vec{k}, t)$ be the non-equilibrium distribution function which describes the probability of

finding the electron at \vec{r} with momentum \vec{k} at time t . $P(t, t')$ denotes the fraction of electrons that are not scattered between times t and t' and satisfies the differential equation

$$\frac{\partial}{\partial t'} P(t, t') = \frac{P(t, t')}{\tau(t')} \quad (1)$$

where $\tau(t) = \tau(\vec{k}(t))$. Integrating this gives

$$P(t, t') = \exp \left(- \int_{t'}^t \frac{du}{\tau(u)} \right). \quad (2)$$

The non-equilibrium distribution function can then be written as

$$g(\vec{r}, \vec{k}, t) = f - \frac{\partial f}{\partial E} \int_{-\infty}^t dt' \vec{E} \cdot \vec{v} P(t, t'), \quad (3)$$

where $f(E)$ is the Fermi function and equals the equilibrium distribution and \vec{E} is the electric field. The conductivity then reduces to

$$\sigma_{ij} = \frac{e^2}{4\pi^3} \int v_i(\vec{k}) \bar{v}_j(\vec{k}) \left(-\frac{\partial f(E)}{\partial E} \right) d^3\vec{k}, \quad (4)$$

where $\bar{v}_j(\vec{k})$ is

$$\bar{v}_j(\vec{k}) = \int_{-\infty}^0 \exp \left[- \int_0^t \frac{du}{\tau(\vec{k}(u))} \right] v_j(\vec{k}(t)) dt \quad (5)$$

and the wave vector $\vec{k}(t)$ satisfies the semi-classical equation of motion

$$\frac{d\vec{k}}{dt} = -\frac{e}{\hbar^2} \vec{\nabla}_k \epsilon(\vec{k}) \times \vec{B}. \quad (6)$$

In a quasi-one dimensional metal the simplest possible dispersion relation is

$$\epsilon(\vec{k}) = \hbar v_F (|k_x| - k_F) - 2t_b \cos(bk_y) - 2t_c \cos(ck_z), \quad (7)$$

where v_F is the Fermi velocity, k_F is the Fermi wave vector, and t_b and t_c are the electron hopping integrals perpendicular to the chains. For the dispersion (7), the interlayer conductivity given by Eq. (4) reduces to

$$\sigma_{zz} = \frac{e^2}{4\pi^3 \hbar v_F} \int_{-\pi/c}^{\pi/c} dk_z(0) \int_0^{2\pi/b} dk_y(0) v_z(\vec{k}) \bar{v}_z(\vec{k}) \quad (8)$$

assuming that the temperature is sufficiently low that the derivative of the Fermi function can be replaced by a delta function at the Fermi energy.

B. Specific model for the scattering rate

The model scattering rate for a quasi-one-dimensional system that we consider is

$$\frac{1}{\tau(k_y)} = \frac{1}{\tau_0} + A \sin^2 \left(\frac{bk_y}{2} \right), \quad (9)$$

where the first term does not vary over the Fermi surface and A is the strength of the cold spots. The second term determines the periodicity of the spots on the Fermi surface (see Fig. 1). This is a quasi-one-dimensional version of the model considered by Ioffe and Millis.⁹ If the cold spots are due to superconducting fluctuations then the superconducting phase would have nodes in the energy gap at $(k_x, k_y) = (\pm k_F, 0)$.

Ioffe and Millis took the scattering time τ_0 to be the sum of an impurity part and a temperature dependent part⁹

$$\frac{1}{\tau_0} = \frac{1}{\tau_{imp}} + \frac{T^2}{T_0}, \quad (10)$$

where T_0 is an energy scale of the order of the Fermi temperature.

C. Zero and high field limits

Zero field limit: The interlayer conductivity, when $\vec{B} = 0$, is given by⁷

$$\sigma_{zz}(B = 0) = \frac{e^2}{4\pi^3} \int \tau(\vec{k}(t)) v_z(\vec{k}) v_z(\vec{k}) d^3\vec{k}, \quad (11)$$

where $f(E)$ is the Fermi function, $\tau(\vec{k})$ the momentum-dependent scattering time and $v_z(\vec{k})$ is the electron velocity perpendicular to the layers. Now in zero magnetic field the velocities are constant thus the conductivity becomes

$$\sigma_{zz}(B = 0) = \frac{e^2}{4\pi^3} \int v_z(k_z)^2 \tau(k_y) \delta(E_F - \epsilon(\vec{k})) d^3\vec{k} = \frac{2e^2 c t_c^2}{\pi \hbar^3 b v_F} \langle \tau \rangle, \quad (12)$$

where $\langle \tau \rangle$ is the average of the lifetime of the carriers on the Fermi surface.

High field limit: At high fields (as $B \rightarrow \infty$) the term $\exp \left[- \int_0^t \frac{du}{\tau(u)} \right]$ in (5) oscillates rapidly, therefore we replace the scattering rate term by its average over the Fermi surface, $\langle \frac{1}{\tau} \rangle$, where $\langle .. \rangle$ denotes the average. Thus we obtain

$$\exp \left[- \int_0^t du \left\langle \frac{1}{\tau} \right\rangle \right] = \exp \left[-t \left\langle \frac{1}{\tau} \right\rangle \right] \quad (13)$$

and evaluating $\bar{v}_z(\vec{k})$ (see Eq. 5) we get

$$\int_0^\infty dt \exp \left[-t \left\langle \frac{1}{\tau} \right\rangle \right] = \frac{1}{\langle \frac{1}{\tau} \rangle}, \quad (14)$$

provided that the velocity, $v_z(\vec{k})$, is independent of the time. The conductivity can then be simplified to

$$\sigma_{zz}(B = \infty) = \frac{2e^2 c t_c^2}{\pi \hbar^3 b v_F} \frac{1}{\langle \frac{1}{\tau} \rangle}. \quad (15)$$

Combining the results for both the high and low field limits gives

$$\frac{\rho_{zz}(B = \infty)}{\rho_{zz}(B = 0)} = \langle \tau \rangle \left\langle \frac{1}{\tau} \right\rangle \quad (16)$$

A similar result was obtained by Zheleznyak and Yakovenko²⁷.

D. Positive Magnetoresistance

By using the Cauchy-Schwarz inequality it can be shown that the right hand side of (16) must be greater than or equal to unity. Thus, the saturating value of the magnetoresistance is always positive. If $f(\vec{k})$ and $g(\vec{k})$ are functions defined on the Fermi surface we can define an inner product

$$(f, g) = \int_{FS} d^2k f(\vec{k}) g(\vec{k}), \quad (17)$$

where the integral is over the Fermi surface. The Cauchy-Schwarz inequality implies that

$$|(f, g)| \leq \|f\| \|g\|, \quad (18)$$

where $\|f\|$ denotes the norm of f defined by $\|f\| = (f, f)^{1/2}$. We set $f(\vec{k}) = \sqrt{\frac{1}{\tau(\vec{k})}}$ and $g(\vec{k}) = \frac{1}{f(\vec{k})}$ and square both sides to obtain

$$1 \leq \int_{FS} \frac{1}{\tau(\vec{k})} d^2k \int_{FS} \tau(\vec{k}) d^2k = \left\langle \frac{1}{\tau(\vec{k})} \right\rangle \langle \tau(\vec{k}) \rangle = \frac{\rho_{zz}(B = \infty)}{\rho_{zz}(B = 0)}. \quad (19)$$

This shows that the resistance at high fields will always be larger than the resistance at zero field. Note that this result does not depend on the particular functional form for the variation of the scattering rate over the Fermi surface.

III. INTERLAYER CONDUCTIVITY IN ZERO FIELD

Substituting the scattering rate (9) and the velocity in the z -axis direction, $v_z = \frac{2ct_c}{\hbar} \sin(ck_z)$, into the conductivity (11), we obtain

$$\sigma_{zz}(B=0) = \frac{e^2}{4\pi^3 \hbar v_F} \left(\frac{2ct_c}{\hbar} \right)^2 \int_{-\pi/c}^{\pi/c} \sin^2(ck_z) dk_z \int_{-\pi/b}^{\pi/b} \frac{dk_y}{\frac{1}{\tau_0} + A \sin\left(\frac{bk_y}{2}\right)^2} . \quad (20)$$

Performing the integrals gives

$$\sigma_{zz}(B=0) = \frac{2e^2 ct_c^2 \tau_0}{\pi \hbar^3 b v_F} \frac{1}{\sqrt{1 + A\tau_0}} \quad (21)$$

and in the absence of cold spots ($A=0$) we get

$$\sigma_{zz}(A=0) = \frac{2e^2 ct_c^2 \tau_0}{\pi \hbar^3 b v_F} . \quad (22)$$

If $1/\tau_0 \sim T^2$, A is independent of temperature and $A\tau_0 \gg 1$ then $\rho_{zz} \sim T$. The different temperature dependences that have been observed in the Bechgaard salts are summarised in Table I.

IV. THE INTERLAYER CONDUCTIVITY IN THE PRESENCE OF A MAGNETIC FIELD

A. Magnetic field parallel to the least conducting axis

We now show how when the field and current are both parallel to the c -axis that the cold spots produce a positive magnetoresistance. For the dispersion relation (7) the components of the group velocity are

$$\vec{v} = \frac{1}{\hbar} \vec{\nabla}_k \epsilon = \frac{1}{\hbar} \begin{pmatrix} \hbar v_F \\ 2bt_b \sin(bk_y) \\ 2ct_c \sin(ck_z) \end{pmatrix} . \quad (23)$$

The rate of change of the wave vector $\vec{k}(t)$, in a magnetic field given by $\vec{B} = (0, 0, B)$, is

$$\frac{d\vec{k}}{dt} = -\frac{e}{\hbar^2} \vec{\nabla}_k \epsilon \times \vec{B} = \frac{1}{\hbar} \begin{pmatrix} -2beBt_b \sin(bk_y)/\hbar \\ ev_F B \\ 0 \end{pmatrix} = \begin{pmatrix} a \\ b \\ c \end{pmatrix} . \quad (24)$$

In order to calculate the time dependence of $\vec{k}(t)$ we integrate Eq. (24), giving

$$k_z(t) = k_z(0) \quad (25)$$

$$k_y(t) = k_y(0) + \frac{\omega_0}{b} t , \quad (26)$$

where

$$\omega_0 = \frac{ev_F B b}{\hbar} \quad (27)$$

is the frequency with which the electron traverses the Fermi surface. The z -component of the group velocity is then

$$v_z = \frac{2ct_c}{\hbar} \sin(ck_z(0)) . \quad (28)$$

Substituting $k_y(t)$ into (9) and evaluating the exponential in (5) we obtain

$$\bar{v}_z(\vec{k}) = v_z(k_z(0)) \exp \left[\frac{A}{2\omega_0} \sin(bk_y(0)) \right] \int_{-\infty}^0 dt \exp \left[\frac{(A\tau_0 + 2)t}{2\tau_0} - \frac{A}{2\omega_0} \sin(bk_y(0) + \omega_0 t) \right] . \quad (29)$$

We introduce the modified Bessel generating function³³ for

$$\begin{aligned} \exp \left[-\frac{A}{2\omega_0} \sin(bk_y(0) + \omega_0 t) \right] &= I_0 \left(-\frac{A}{2\omega_0} \right) + 2 \sum_{k=0}^{\infty} (-1)^k I_{2k+1} \left(-\frac{A}{2\omega_0} \right) \sin((2k+1)(bk_y(0) + \omega_0 t)) \\ &+ 2 \sum_{k=1}^{\infty} (-1)^k I_{2k} \left(-\frac{A}{2\omega_0} \right) \cos((2k)(bk_y(0) + \omega_0 t)) \end{aligned} \quad (30)$$

and perform the integral over t to obtain

$$\begin{aligned} \bar{v}_z(\vec{k}) &= v_z(k_z(0)) \exp \left[\left(-\frac{A}{2\omega_0} \right) \sin(bk_y(0)) \right] \left\{ \frac{I_0 \left(-\frac{A}{2\omega_0} \right)}{C} \right. \\ &+ 2 \sum_{k=0}^{\infty} (-1)^k I_{2k+1} \left(-\frac{A}{2\omega_0} \right) \left[\frac{-(2k+1)\omega_0 \cos(b(2k+1)k_y(0)) + C \sin(b(2k+1)k_y(0))}{C^2 + (2k+1)^2 \omega_0^2} \right] \\ &\left. + 2 \sum_{k=1}^{\infty} (-1)^k I_{2k} \left(-\frac{A}{2\omega_0} \right) \left[\frac{(2k)\omega_0 \sin(b(2k)k_y(0)) + C \cos(b(2k)k_y(0))}{C^2 + (2k)^2 \omega_0^2} \right] \right\}, \end{aligned} \quad (31)$$

where $C = \frac{A\tau_0+2}{2\tau_0}$. A similar substitution can be made for the $\exp \left[\frac{A}{2\omega_0} \sin(bk_y(0)) \right]$ term in (31) by setting $t = 0$ in (30). Multiplying out all terms, we note that the only terms that survive the integral over $k_y(0)$ are those whose indicies in the summations are equal. Performing the integrals in $k_y(0)$ and $k_z(0)$ the conductivity becomes

$$\frac{\sigma_{zz}(B)}{\sigma_{zz}(A=0)} = \frac{1}{(1 + \frac{A\tau_0}{2})} \sum_{k=-\infty}^{\infty} \frac{(-1)^k I_k \left(\frac{A}{2\omega_0} \right)^2}{1 + \frac{4k^2 \omega_0^2 \tau_0^2}{(2 + A\tau_0)^2}}. \quad (32)$$

In the Appendix we present an alternative form for this expression that is more stable for numerical evaluation. Fig. 2 shows the dependence of the interlayer resistivity on the strength of the magnetic field at various values of the parameter $A\tau_0$.

High field limit: The conductivity, as $\frac{A}{\omega_0} \rightarrow 0$, is simplified by the limiting form for small arguments of the modified Bessel function

$$I_k(z) \sim \frac{\left(\frac{1}{2}z\right)^k}{\Gamma(k+1)} \quad (k \neq -1, -2, \dots) \quad (33)$$

and so the $k = 0$ term dominates (32) giving

$$\frac{\rho_{zz}(\omega_0 \gg A)}{\rho_{zz}(A=0)} = 1 + \frac{A\tau_0}{2}. \quad (34)$$

This agrees with the general result (15).

B. Magnetic field parallel to the b -axis

Chashechkina and Chaikin found that for $(\text{TMTSF})_2\text{ClO}_4$ under 6 kbar pressure²⁵, the interlayer resistivity (for field directed along the b -axis) deviates from the quadratic field dependence which is predicted from simple Boltzmann transport theory. Although it is quadratic at low fields the resistivity becomes approximately linear at higher fields. Kohler's rule is obeyed. In contrast, for $(\text{TMTSF})_2\text{PF}_6$ at 10 kbar the interlayer resistivity saturates above fields of about 2 tesla^{34,35}.

With a magnetic field given by $\vec{B} = (0, B, 0)$ the rate of change of the wave vector is $d\vec{k}/dt = (\frac{2eBct_c \sin(ck_z)}{\hbar^2}, 0, -\frac{ev_F B}{\hbar})$. From this the z -axis velocity is calculated to be $v_z(k_z) = \frac{2ct_c}{\hbar} \sin(ck_z(0) - \omega_0 t)$, where $\omega_0 c = c\omega_0/b$. In this case, when the magnetic field is parallel to the b -axis, k_y is constant and so τ is not a function of time. Thus the electron trajectories are either in or out of the cold spot region, but never swept through them. One can write Eq. (5) as

$$\bar{v}_z(\vec{k}) = \int_{-\infty}^0 dt v_z(\vec{k}(t)) \exp\left[-\frac{t}{\tau(k_y)}\right]. \quad (35)$$

After the appropriate substitution for the scattering rate and z -axis velocity we obtain

$$\bar{v}_z(\vec{k}) = \frac{2ct_c}{\hbar} \left[\frac{\omega_0 \cos(ck_z(0)) - R \sin(ck_z(0))}{R^2 + \omega_0^2} \right], \quad (36)$$

where $R = \frac{1}{\tau_0} + A \sin\left(\frac{bk_y(0)}{2}\right)^2$ and for simplicity here we set $b = c$ so $\omega_{0c} = \omega_0$. The conductivity can then be written as

$$\sigma_{zz}(B) = \frac{e^2}{4\pi^3 \hbar v_F b} \left(\frac{2ct_c}{\hbar}\right)^2 \int_0^{2\pi/b} dk_y(0) \int_0^{2\pi/c} dk_z(0) \sin(ck_z(0)) \left[\frac{\omega_0 \cos(ck_z(0)) - R \sin(ck_z(0))}{R^2 + \omega_0^2} \right]. \quad (37)$$

Performing the integral over $dk_z(0)$ we obtain

$$\sigma_{zz}(B) = \frac{e^2}{4\pi^2 c \hbar v_F b} \left(\frac{2ct_c}{\hbar}\right)^2 \int_0^{2\pi/b} dk_y(0) \frac{\left(\frac{1}{\tau_0} + A \sin\left(\frac{bk_y(0)}{2}\right)^2\right)}{\left(\frac{1}{\tau_0} + A \sin\left(\frac{bk_y(0)}{2}\right)^2\right)^2 + \omega_0^2} \quad (38)$$

and integrate to give

$$\frac{\sigma_{zz}(B)}{\sigma_{zz}(A=0)} = \frac{\sin\left(\frac{\arctan\left(\frac{1}{\omega_0\tau_0}\right) + \arctan\left(\frac{1+A\tau_0}{\omega_0\tau_0}\right)}{2}\right)}{[1 + (\omega_0\tau_0)^2]^{1/4} [(1 + A\tau_0)^2 + (\omega_0\tau_0)^2]^{1/4}}. \quad (39)$$

High field limit: If $\omega_0 \gg 1/\tau_0$ and $\omega_0 \gg A$ we can expand in $\frac{1}{\omega_0\tau_0}$ to second order to obtain

$$\frac{\sigma_{zz}(B)}{\sigma_{zz}(A=0)} = \frac{2 + A\tau_0}{2} \frac{1}{(\omega_0\tau_0)^2}. \quad (40)$$

Thus, at high fields the resistivity is quadratic in field and does not saturate. This is inconsistent with the experimental results on TMTSF₂X cited above.

Low field limit: Here we expand in $\omega_0\tau_0$ to second order to obtain

$$\frac{\sigma_{zz}(\omega_0\tau_0 \ll 1)}{\sigma_{zz}(A=0)} = \frac{1}{\sqrt{1 + A\tau_0}} - \frac{(8 + A\tau_0(8 + 3A\tau_0))}{8(1 + A\tau_0)^{5/2}} (\omega_0\tau_0)^2, \quad (41)$$

where we can write, after simplifying, the resistivity as

$$\frac{\rho_{zz}(B)}{\rho_{zz}(A=0)} = \sqrt{1 + A\tau_0} \left(1 + \frac{(8 + A\tau_0(8 + 3A\tau_0))(\omega_0\tau_0)^2}{8(1 + A\tau_0)^2}\right) \quad (42)$$

A comparison of the result (39) with the quadratic form (42) is shown in Fig. 3, for $A\tau_0 = 1, 10$. In the absence of cold spots Boltzmann transport theory predicts a quadratic field dependence for all fields. The plot shows that the quadratic fit (dashed line) deviates from the exact solution (solid line) at large fields. As the strength of the cold spots increase the deviations increase further, while the exact solution becomes increasingly linear at small fields. Note that the low-field quadratic fit always lies above the actual result, as is observed in (TMTSF)₂ClO₄ at 6 kbar.²⁵

Kohler's rule: Equation (39) shows that the resistance depends on three parameters: ω_0 which is linearly proportional to the magnetic field, the scattering time τ_0 and A the parameter that determines the strength of the cold spots. Since τ_0 and A can both depend on temperature, we can analyse the temperature and field dependence of the magnetoresistance in terms of Kohler's rule³⁶. Kohler's rule is known to hold when there is a single species of charge carrier and the scattering time τ is the same at all points on the Fermi surface²². The dependence of the resistivity on the field in (39) is contained in the quantity $\omega_0\tau_0$ and the temperature dependence of $A\tau_0$. In zero field the conductivity is given by (21). The field dependence of the magnetoresistance, with different scattering times, can be related by scaling the field by the zero-field resistivity $\rho_{zz}(B=0, A\tau_0)$. To obtain a Kohler's plot we plot $\frac{\rho_{zz}(B, A\tau_0)}{\rho_{zz}(B=0, A\tau_0)}$ versus $\frac{B}{\rho_{zz}(B=0, A\tau_0)}$. In order to do this we re-arrange Eq. (39) to give

$$\frac{\sigma_{zz}(B, A\tau_0)}{\sigma_{zz}(B=0, A\tau_0)} = \frac{\sin\left(\frac{\arctan\left(\frac{1}{\omega_0\tau_0}\right) + \arctan\left(\frac{1+A\tau_0}{\omega_0\tau_0}\right)}{2}\right)}{[1 + (\omega_0\tau_0)^2]^{1/4} \left[1 + \frac{(\omega_0\tau_0)^2}{(1+A\tau_0)^2}\right]^{1/4}}, \quad (43)$$

and plot the inverse of this against $\omega_0\tau_0/\sqrt{1+A\tau_0}$, because $\rho_{zz}(B=0, A\tau_0) \propto \sqrt{1+A\tau_0}/\tau_0$. Fig. 4 shows such a plot for various values of $A\tau_0$. The figure shows that Kohler's rule is violated at high fields and for $A\tau_0 \gtrsim 5$; if it held all the curves would collapse onto a single curve.

C. Magnetic field in the $b-c$ plane

For rotations of the magnetic field in the $b-c$ plane experiments on $(\text{TMTSF})_2\text{ClO}_4$ at ambient²⁴ and 6 kbar²⁵ pressure and $(\text{TMTSF})_2\text{PF}_6$ at 6 kbar³⁵ find that the angular dependence of the interlayer magnetoresistance has dips at the magic angles superimposed on roughly the angular dependence predicted by semi-classical transport theory. The magnetoresistance is minimum when the magnetic field and the current are parallel and a maximum when the field and current are perpendicular. This is in contrast to the anomalous behaviour seen in $(\text{TMTSF})_2\text{PF}_6$ at 10 kbar^{21,34} where the opposite is observed: the background magnetoresistance only depends on the component of the field perpendicular to the layers, $\rho_{zz} \sim (B \cos \theta)^{1.3}$.

Following a similar procedure as in Section IV A the rate of change of the wave vector, in a magnetic field given by $\vec{B} = (0, B \sin \theta, B \cos \theta)$, is

$$\frac{d\vec{k}}{dt} = -\frac{e}{\hbar^2} \vec{\nabla}_k \epsilon \times \vec{B} = \frac{1}{\hbar^2} \begin{pmatrix} -2beBt_b \cos \theta \sin(bk_y) \\ ev_F \hbar B \cos \theta \\ -ev_F \hbar B \sin \theta \end{pmatrix} \begin{pmatrix} a \\ b \\ c \end{pmatrix}. \quad (44)$$

The velocity in the c -direction (z -axis) can then be written

$$v_z(k_z) = \frac{2ct_c}{\hbar} \sin(ck_z(0) - \omega_c t) \quad (45)$$

and $\bar{v}_z(\vec{k})$, from Eq. (5), can be calculated by making the appropriate substitutions for the scattering rate and the c -axis velocity, giving

$$\bar{v}_z(\vec{k}) = \frac{2ct_c}{\hbar} \exp\left[\frac{A}{2\omega_B} \sin(bk_y(0))\right] \int_{-\infty}^0 dt \sin(ck_z(0) - \omega_c t) \exp\left[\left(\frac{A\tau_0 + 2}{2\tau_0}\right)t - \frac{A}{2\omega_B} \sin(bk_y(0) + \omega_B t)\right], \quad (46)$$

where $\omega_B = \frac{ebBv_F \cos \theta}{\hbar} = \omega_0 \cos \theta$ and $\omega_c = \frac{ecBv_F \sin \theta}{\hbar}$. Substitution of the appropriate modified Bessel generating functions and performing the integral over t gives

$$\begin{aligned} \bar{v}_z(\vec{k}) = & \frac{2ct_c}{\hbar} \exp\left[\left(-\frac{A}{2\omega_B}\right) \sin(bk_y(0))\right] \left\{ I_0\left(-\frac{A}{2\omega_B}\right) \left[\frac{\omega_c \cos(ck_z(0)) + C \sin(ck_z(0))}{C^2 + \omega_c^2}\right] \right. \\ & + \sum_{k=0}^{\infty} (-1)^k I_{2k+1}\left(-\frac{A}{2\omega_B}\right) \left[\frac{C \cos(ck_z(0) - (2k+1)bk_y(0)) - ((2k+1)\omega_B + \omega_c) \sin(ck_z(0) - (2k+1)bk_y(0))}{C^2 + ((2k+1)\omega_B + \omega_c)^2}\right. \\ & \quad \left. - \frac{C \cos(ck_z(0) + (2k+1)bk_y(0)) - ((2k+1)\omega_B - \omega_c) \sin(ck_z(0) + (2k+1)bk_y(0))}{C^2 + (-(2k+1)\omega_B + \omega_c)^2}\right] \\ & + \sum_{k=1}^{\infty} (-1)^k I_{2k}\left(-\frac{A}{2\omega_B}\right) \left[\frac{C \sin(ck_z(0) - (2k)bk_y(0)) + ((2k)\omega_B - \omega_c) \cos(ck_z(0) - (2k)bk_y(0))}{C^2 + (2k\omega_B + \omega_c)^2}\right. \\ & \quad \left. + \frac{C \sin(ck_z(0) + (2k)bk_y(0)) + ((2k)\omega_B + \omega_c) \cos(ck_z(0) + (2k)bk_y(0))}{C^2 + (-(2k)\omega_B + \omega_c)^2}\right] \Big\}, \end{aligned} \quad (47)$$

where $C = \frac{1}{\tau_0} + \frac{A}{2}$. Performing the integrals over $k_y(0)$ and $k_z(0)$ one obtains

$$\frac{\sigma_{zz}(B)}{\sigma_{zz}(A=0)} = \left(\frac{1}{1 + \frac{A\tau_0}{2}}\right) \sum_{k=-\infty}^{\infty} \frac{(-1)^k I_k\left(\frac{A}{2\omega_B}\right)^2}{1 + \frac{4\tau_0^2(k\omega_B + \omega_c)^2}{(2+A\tau_0)^2}}. \quad (48)$$

Based on this expression we expect to see features in the angular dependence when

$$k = \frac{\omega_c}{\omega_B} = \frac{c}{b} \tan \theta . \quad (49)$$

Due to the alternating sign in the summation, when the index k is even one expects to see dips, while when k is odd one expects peaks in the resistivity. A plot of the interlayer resistivity versus the field tilt angle θ is shown in Fig. 5 for several parameter values. It can be seen that only the $k = 1$ resonance is noticeable, and only for very large fields ($\omega_0\tau_0 > 100$). Experimentally the magic angle effects are seen at much lower fields. Furthermore, one always sees dips and not peaks at the magic angles.

V. CONDUCTIVITY PARALLEL TO THE CHAINS

Measurements of the resistivity parallel to the a axis for rotations of the magnetic field in the $b - c$ plane show similar behavior as for the interlayer resistivity^{24,25,21,34}. Magic angle effects are superimposed on a background magnetoresistance which has a semiclassical angular dependence for (TMTSF)₂ClO₄ and is anomalous for (TMTSF)₂PF₆ at 10 kbar. For the latter a power law field dependence of the a -axis resistivity was found with the field in the c -axis direction by Kriza *et al.*³⁷, $\rho_{xx}(B) - \rho_{xx}(0) \propto B^{3/2}$.

The conductivity parallel to the chains (σ_{xx}) is calculated in a similar manner to the interlayer conductivity, where the magnetic field is rotated in the $b - c$ plane. Calculating the velocity in the x -axis direction ($v_x = v_F$), we can substitute this and our specific model for the scattering rate into Eq. (4) and (5) to obtain

$$\begin{aligned} \sigma_{xx} = & \frac{e^2}{4\pi^3\hbar v_F} \int_0^{2\pi/c} dk_z(0) \int_0^{2\pi/b} dk_y(0) v_F \exp \left[\frac{A}{2\omega_B} \sin(bk_y(0)) \right] \\ & \times \int_{-\infty}^0 dt v_F \exp \left[\frac{(A\tau_0 + 2)t}{2\tau_0} - \frac{A}{2\omega_B} \sin(bk_y(0) + \omega_B t) \right] . \end{aligned} \quad (50)$$

Performing the integral and simplifying we obtain

$$\frac{\sigma_{xx}}{\sigma_{xx}(A=0)} = \left(\frac{1}{1 + \frac{A\tau_0}{2}} \right) \sum_{k=-\infty}^{\infty} \frac{(-1)^k I_k \left(\frac{A}{2\omega_0 \cos \theta} \right)^2}{1 + \frac{4(k\tau_0\omega_0 \cos \theta)^2}{(2 + A\tau_0)^2}} . \quad (51)$$

Note that for $\theta = 0$ this will give the same field dependence for the conductivity in the least conducting direction (compare Eq. 32 and Fig. 2).

The angular dependence of the resistivity $\rho_{xx} \equiv 1/\sigma_{xx}$ given by the equation above is plotted in Fig. 6 for two values of $A\tau_0$ and $\omega_0\tau_0$. We see that some similarities exist between theory and experimental results on (TMTSF)₂PF₆ at 9.5 kbar pressure for rotations of the magnetic field in the $b - c$ plane^{34,38}, in that the resistivity is large for magnetic field angles close to $\theta=0^\circ$ and decreases as θ approaches 90° . Furthermore, the resistivity only depends on the component of field perpendicular to the layers; that is, $\omega_B = \omega_0 \cos \theta$. We tried fitting the field dependence to a power law of the form $\rho_{xx} \sim (B \cos \theta)^\alpha$ but found this only applied over very limited field ranges. The calculated angular dependence of ρ_{xx} also differs from the observed angular dependence in that no magic angle features are present in the calculated $\rho_{xx}(\theta)$.

VI. CONCLUSION

We have considered a modification of standard Fermi liquid and Boltzmann transport theory in which there are large variations of the quasiparticle scattering rate over a quasi-one-dimensional Fermi surface. The goal was to see to what extent such a model could explain the anomalous properties of the magnetoresistance of the quasi-one-dimensional organic metals, (TMTSF)₂X. Table I gives a brief comparison of the results of our calculations for a cold spots model with experimental results. Although the model can explain a number of unusual features such as having a large magnetoresistance when the field and current are parallel there are several important discrepancies. Although the model does give magic angle effects they are orders of magnitude smaller than is observed experimentally. In particular explaining the origin of the magic angle effect and why in (TMTSF)₂PF₆ at 10 kbar the interlayer resistivity becomes independent of field for fields parallel to the b axis remains a considerable challenge.

ACKNOWLEDGMENTS

We thank L. Ioffe and J. Merino for helpful discussions. This work was supported by the Australian Research Council.

APPENDIX A: ALTERNATIVE EXPRESSION FOR CONDUCTIVITY

We now derive an alternative expression for Eq. (32) which is more stable for numerical evaluation. One can re-write the conductivity in (4), using (28) and (29), as

$$\sigma_{zz} = \frac{e^2}{4\pi^3 \hbar v_F} \left(\frac{2ct_c}{\hbar} \right)^2 \int_{-\pi/c}^{\pi/c} dk_z(0) \sin(ck_z(0)) \int_0^{2\pi/b} dk_y(0) \exp \left[\frac{A}{2\omega_0} \sin(bk_y(0)) \right] \times \int_{-\infty}^0 dt \sin(ck_z(0)) \exp \left[\frac{(A\tau_0 + 2)t}{2\tau_0} - \frac{A}{2\omega_0} \sin(bk_y(0) + \omega_0 t) \right]. \quad (\text{A1})$$

Since $\sin(bk_y(0) + \omega_0 t)$ is periodic in t we can divide the range of integration into segments of length $\frac{2\pi}{\omega_0}$ and sum the resulting geometric series giving

$$\sigma_{zz} = \frac{ce^2}{4\pi^2 \hbar v_F} \left(\frac{2t_c}{\hbar} \right)^2 \frac{1}{1 - \exp \left(-\frac{\pi(A\tau_0 + 2)}{\omega_0 \tau_0} \right)} \int_0^{2\pi/b} dk_y(0) \exp \left[\frac{A}{2\omega_0} \sin(bk_y(0)) \right] \times \int_0^{2\pi} \frac{d\phi}{\omega_0} \exp \left[-\frac{(A\tau_0 + 2)}{2\tau_0} \frac{\phi}{\omega_0} - \frac{A}{2\omega_0} \sin(bk_y(0) + b\phi) \right], \quad (\text{A2})$$

where $\phi = \omega_0 t$. Shifting the integration over $k_y(0)$ by $-\phi/2$ and re-arranging terms we obtain

$$\sigma_{zz} = \frac{ce^2}{4\pi^2 \hbar v_F} \left(\frac{2t_c}{\hbar} \right)^2 \frac{1}{1 - \exp \left(-\frac{\pi(A\tau_0 + 2)}{\omega_0 \tau_0} \right)} \int_0^{2\pi/b} dk_y(0) \exp \left[\frac{A}{2\omega_0} (\sin(bk_y(0) - \phi/2) - \sin(bk_y(0) + \phi/2)) \right] \times \int_0^{2\pi} \frac{d\phi}{\omega_0} \exp \left[-\frac{(A\tau_0 + 2)\phi}{2\omega_0 \tau_0} \right] \quad (\text{A3})$$

which upon simplification and performing the integration over $k_y(0)$ gives

$$\frac{\sigma_{zz}(B)}{\sigma_{zz}(0)} = \left(\frac{1}{\omega_0 \tau_0} \right) \frac{1}{1 - \exp \left(-\frac{\pi(A\tau_0 + 2)}{\omega_0 \tau_0} \right)} \int_0^{2\pi} d\phi \, I_0 \left(\frac{A\tau_0}{\omega_0 \tau_0} \sin(\phi/2) \right) \exp \left[-\frac{(A\tau_0 + 2)\phi}{2\omega_0 \tau_0} \right]. \quad (\text{A4})$$

* New address: Department of Physics, University of Queensland, Brisbane, 4072, Australia; e-mail: mckenzie@physics.uq.edu.au

¹ P. W. Anderson, *The Theory of Superconductivity in the High T_c Cuprates* (Princeton U.P., Princeton, 1997).

² For a recent experimental review, see W. Y. Liang, J. Phys.: Condens. Matter **10**, 11365 (1998).

³ L. Degiorgi, Rev. Mod. Phys. **71**, 687 (1999).

⁴ J. Wosnitzer, *Fermi Surfaces of Low Dimensional Organic Metals and Superconductors* (Springer, Berlin, 1996).

⁵ R. H. McKenzie, Comments Cond. Mat. Phys. **18**, 309 (1998).

⁶ C. Bourbonnais and D. Jerome, cond-mat/9903101.

⁷ N. W. Ashcroft and N. D. Mermin, *Solid State Physics* (Saunders, Philadelphia, 1975).

⁸ D. Pines, Physica C **282**, 273 (1997).

⁹ L. B. Ioffe and A. J. Millis, Phys. Rev. B **58**, 11631 (1998).

¹⁰ N. D. Mathur, F. M. Grosche, S. R. Julian, I. R. Walker, D. M. Freye, R. K. W. Haselwimmer and G. G. Lonzarich, Nature **394**, 39 (1998).

- ¹¹ P. Coleman, Physica B **261**, 353 (1999).
- ¹² J. L. Smith and Q. Si, Europhys. Lett. **45**, 228 (1999).
- ¹³ A. Rosch, Phys. Rev. Lett. **82**, 4280 (1999).
- ¹⁴ S. P. Strong, D. G. Clarke, and P. W. Anderson, Phys. Rev. Lett. **73**, 1007 (1994); D. G. Clarke and S. P. Strong, Adv. Phys. **46**, 545 (1997).
- ¹⁵ A. T. Zheleznyak and V. M. Yakovenko, Eur. Phys. J. B **11**, 385 (1999).
- ¹⁶ K. Maki, Phys. Rev. B. **45**, 5111 (1992); R. H. McKenzie and P. Moses, cond-mat/0006220.
- ¹⁷ T. Osada, S. Kagoshima and N. Miura, Phys. Rev. B. **46**, 1812 (1992).
- ¹⁸ S. J. Blundell and J. Singleton, Phys. Rev. B **53**, 5609 (1996).
- ¹⁹ A. G. Lebed and P. Bak, Phys. Rev. Lett. **63**, 1315 (1989).
- ²⁰ P. M. Chaikin, Phys. Rev. Lett. **69**, 2831 (1992).
- ²¹ D. G. Clarke, S. P. Strong, P. M. Chaikin and E. I. Chashechkina, Science **279**, 2071 (1998).
- ²² R. H. McKenzie, J. S. Qualls, S. Y. Han and J. S. Brooks, Phys. Rev. B. **57**, 11854 (1998).
- ²³ J. S. Qualls, J. S. Brooks, S. Uji, T. Terashima, C. Terakura, H. Aoki and L. K. Montgomery, cond-mat/0005202.
- ²⁴ G. Danner, W. Kang and P. M. Chaikin, Physica B **201**, 442 (1994).
- ²⁵ E. I. Chashechkina and P. M. Chaikin, Phys. Rev. B **56**, 13658 (1997).
- ²⁶ G. M. Danner, N. P. Ong, and P. M. Chaikin, unpublished.
- ²⁷ A. T. Zheleznyak and V. M. Yakovenko, Synth. Metals **70**, 1005 (1995).
- ²⁸ A. Carrington, A. P. Mackenzie, C. T. Lin and J. R. Cooper, Phys. Rev. Lett. **69**, 2855 (1992).
- ²⁹ B. P. Stojkovic and D. Pines, Phys. Rev. Lett. **76**, 811 (1996).
- ³⁰ R. Hlubina and T. M. Rice, Phys. Rev. B **51**, 9253 (1995).
- ³¹ A. T. Zheleznyak, V. M. Yakovenko, and H. D. Drew, Phys. Rev. B **59**, 207 (1999).
- ³² D. van der Marel, Phys. Rev. B **60**, R765 (1999).
- ³³ M. Abramowitz and I. A. Stegun, *Handbook of Mathematical Functions*, (Dover, New York, 1972).
- ³⁴ E. I. Chashechkina and P. M. Chaikin, Phys. Rev. Lett. **80**, 2181 (1998).
- ³⁵ I. J. Lee and M. J. Naughton, Phys. Rev. B **58**, R13343 (1998).
- ³⁶ A. B. Pippard, *Magnetoresistance in Metals*, (Cambridge University Press, Cambridge, 1989).
- ³⁷ G. Kriza, G. Szeghy, I. Kezsmarki and G. Mihaly, Phys. Rev. B **60**, R8434 (1999).
- ³⁸ G. M. Danner and P. M. Chaikin, Phys. Rev. Lett. **75**, 4690 (1995).
- ³⁹ B. Korin-Hamzic, L. Forro, J. R. Cooper and K. Bechgaard, Phys. Rev. B **38**, 11177, (1988).
- ⁴⁰ J. Moser, M. Gabay, P. Auban-Senzier, D. Jerome, K. Bechgaard and J. M. Fabre, Euro. Phys. J. B **1**, 39 (1998).
- ⁴¹ J. Moser, J. R. Cooper, D. Jerome, B. Alavi, S. E. Brown and K. Bechgaard, Phys. Rev. Lett. **84**, 2674 (2000).
- ⁴² G. Mihaly, I. Kezsmarki, F. Zamborszky and L. Forro, Phys. Rev. Lett. **84**, 2670 (2000).
- ⁴³ L. P. Gor'kov and M. Mochena, Phys. Rev. B **57**, 6204 (1998).

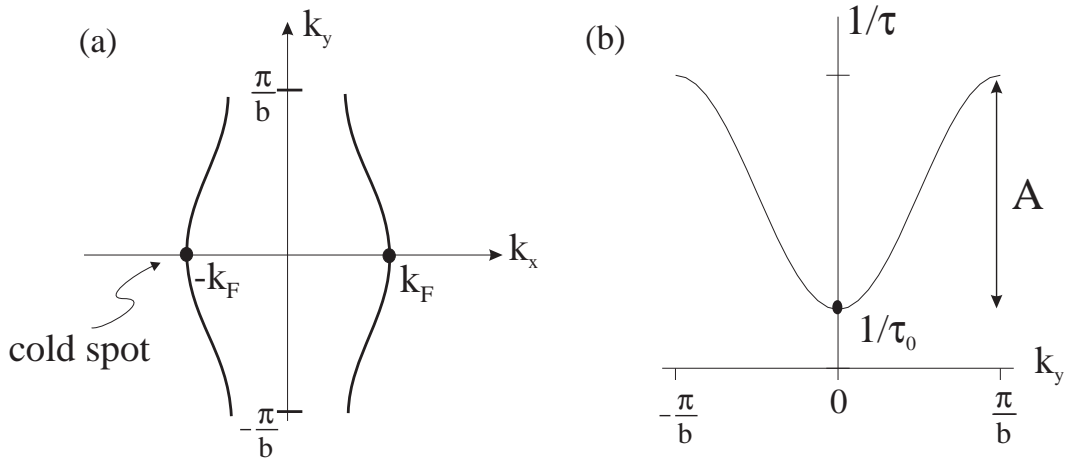


FIG. 1. (a) Cold spots on the intra-layer Fermi surface in a quasi-one-dimensional metal. For a three dimensional Fermi surface the cold spots become cold strips. A magnetic field perpendicular to the layers causes electrons on the Fermi surface to be swept in and out of the cold spots. (b) Variation of the scattering rate across the Fermi surface. The strength of the scattering rate at the cold spot is $\frac{1}{\tau_0}$ and increases by A at the edges of the Brillouin zone.

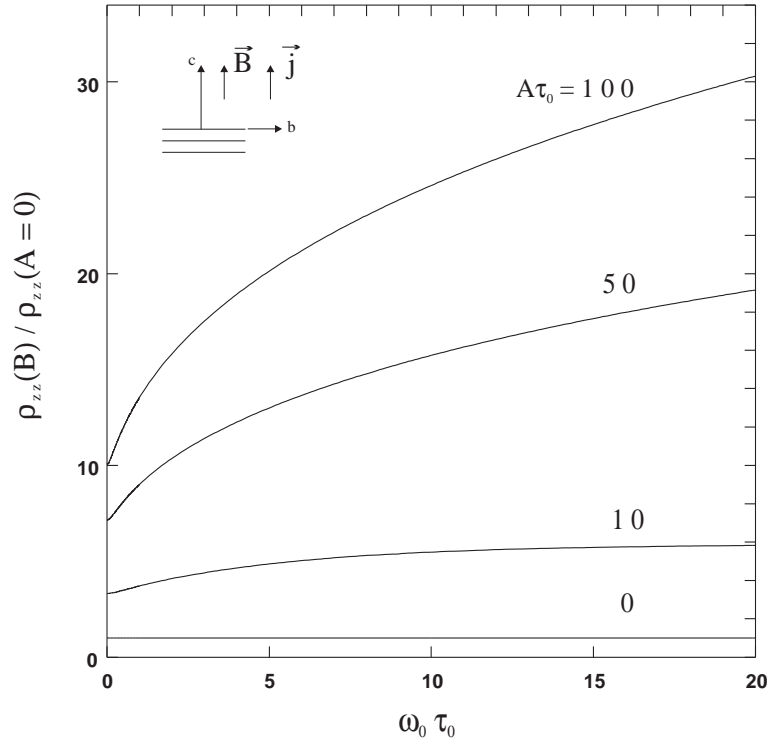


FIG. 2. Dependence of interlayer resistivity on the strength of the magnetic field at various values of the parameter $A\tau_0$, which is a measure of the strength of the scattering cold spots. The magnetic field is perpendicular to the layers and parallel to the current direction and the c -axis (see inset). In the absence of cold spots ($A = 0$) the resistivity is independent of the field. As the strength of the cold spots increases the magnetoresistance increases and is positive and non-zero. For high magnetic fields ($\omega_0 \gg A$) the resistivity saturates to a value given by Eq. (34).

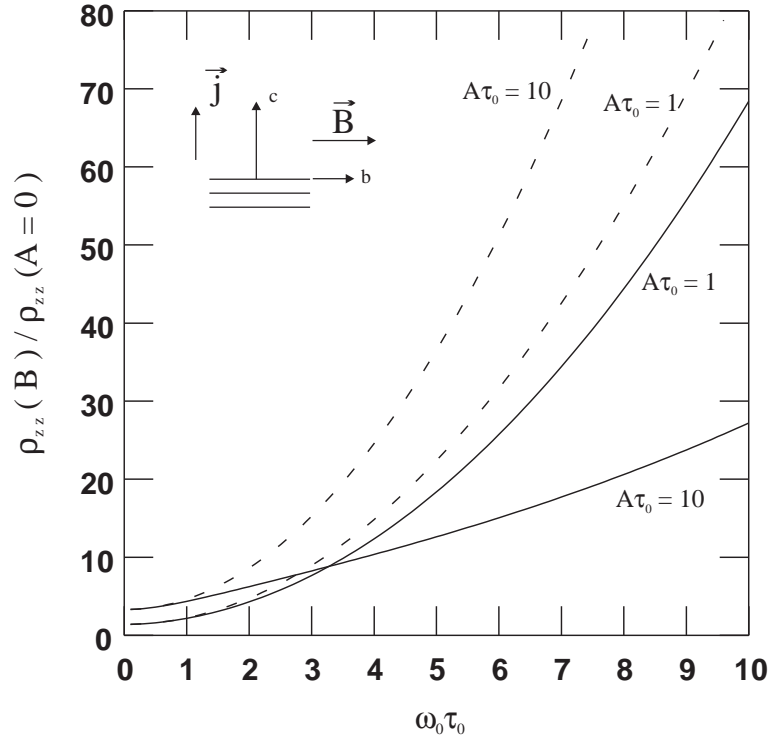


FIG. 3. Field dependence of the interlayer magnetoresistance when the magnetic field is parallel to the b -axis. The exact solution (solid line) and the quadratic fit to the low field magnetoresistance (dashed line), are compared. The quadratic form, as predicted from a simple Boltzmann model²⁵ does not fit the exact form at high fields. This can be compared to experimental results on $(\text{TMTSF})_2\text{ClO}_4$ at 6 kbar²⁵. Deviations from the quadratic form arise due to the variation of the scattering rate over the Fermi surface. As the strength of the cold spots increases the deviation of the low-field fit from the exact solution increases and the exact solution becomes increasingly linear at small fields. Also note that the quadratic form lies above the exact solution at all values of $A\tau_0$.

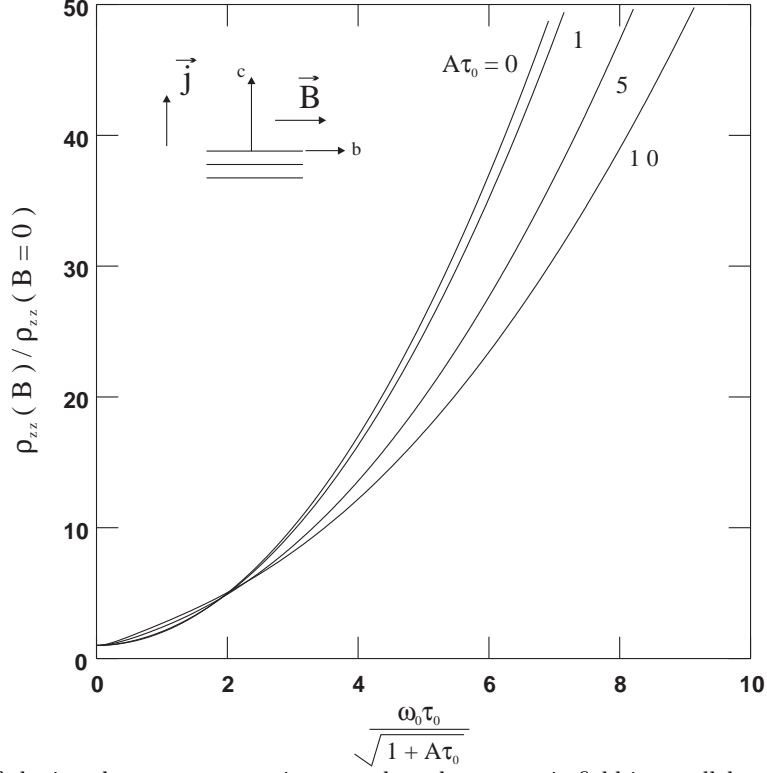


FIG. 4. Kohler's plot of the interlayer magnetoresistance when the magnetic field is parallel to the b -axis. Plots are shown for various values of $A\tau_0$, a quantity that can depend on temperature. The horizontal axis is proportional to $\frac{B}{\rho_{zz}(B=0)}$. We see that Kohler's rule is violated since all the curves do not lie on top of each other. However, the violations are only significant for large magnetic fields and if the cold spots are sufficiently strong that $A\tau_0 \geq 5$.

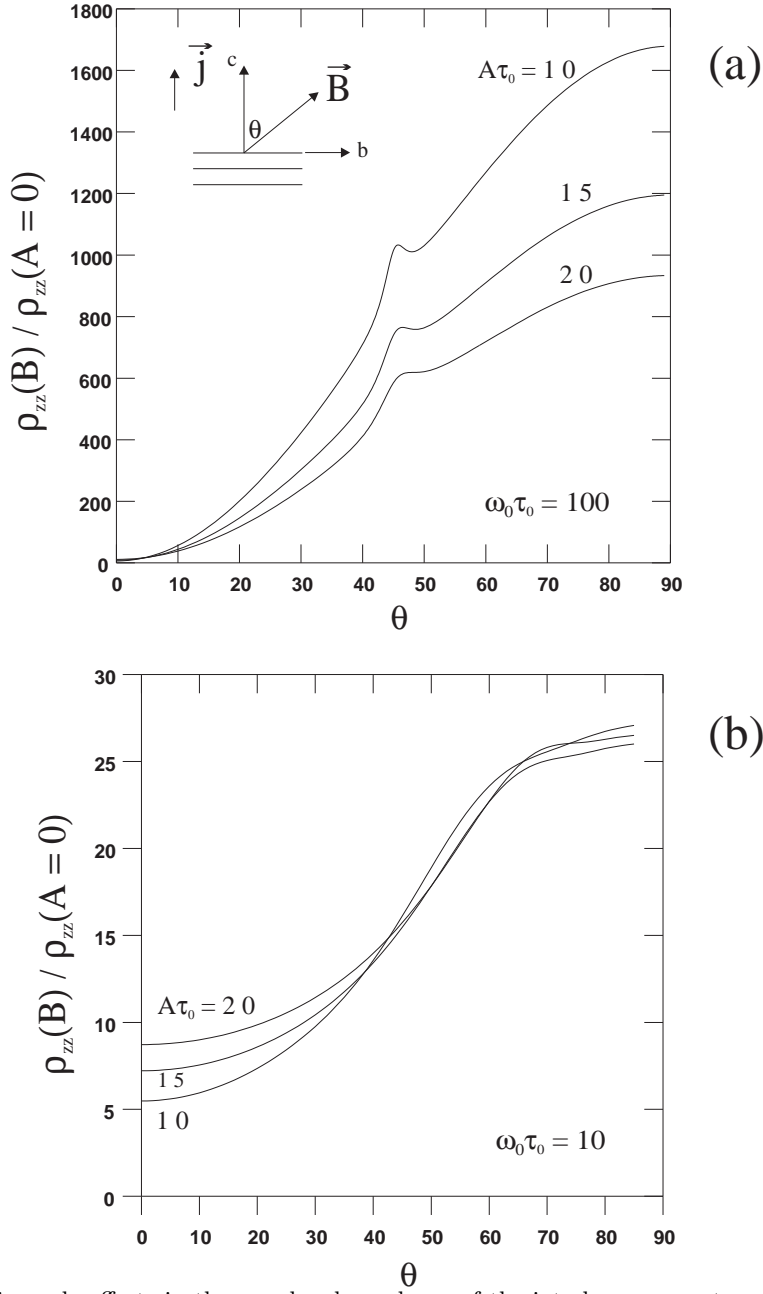


FIG. 5. Absence of magic angle effects in the angular dependence of the interlayer magnetoresistance. The dependence of the interlayer resistivity on the magnetic field direction (rotated in the $b - c$ plane) is shown for various values of $A\tau_0$ and two values of $\omega_0\tau_0$ which is proportional to the strength of the magnetic field. θ is the angle between the most conducting direction (c -axis) and the magnetic field (see inset of (a)). In contrast to experimental results on the quasi-one dimensional metals $(\text{TMTSF})_2\text{X}$ one sees a peak rather than a dip, at $\tan \theta = \frac{b}{c}$. Furthermore, features at higher order magic angles ($\tan \theta = \frac{nb}{c}$ where $n = 2, 3, \dots$) are too small to be visible.

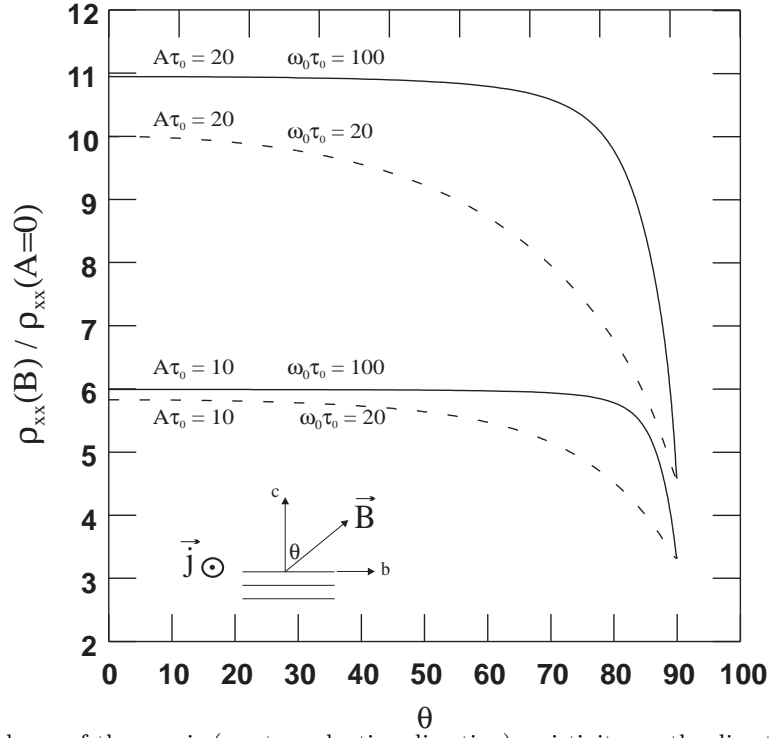


FIG. 6. Angular dependence of the x -axis (most conducting direction) resistivity on the direction of the magnetic field in the $b - c$ plane. In comparison to experimental data on $(\text{TMTSF})_2\text{PF}_6$ at 9.5 kbar pressure^{34,38}, we see a similarity in that the interlayer resistance only depends on the component of field parallel to the c axis and decreases with increasing angle. However, no features are present at the magic angles.

TABLE I. Comparison of the observed properties of the magnetoresistance of $(\text{TMTSF})_2\text{X}$ with the theoretical cold spot model.

Effect	X= ClO_4 (ambient)	X= PF_6 (9-11 kbar)	Cold spot model
Magic angle effect in ρ_{xx}	yes	yes	no
Magic angle effect in ρ_{zz}	yes	yes	yes: but too weak
Peaks rather than dips for odd integers	no	no	yes
Background magnetoresistance only depends on $\cos \theta$	no	yes	yes: ρ_{xx} , no: ρ_{zz}
Violations of Kohler's rule	no	yes	yes

TABLE II. The temperature dependence of the zero-field resistivity of $(\text{TMTSF})_2\text{X}$ at various pressures. We also show if the classical angular dependence curve is observed in the particular materials.

X	pressure	Classical angular dependence	$\rho_{zz}(B=0, T)$	$\rho_{xx}(B=0, T)$
ClO_4	ambient	Yes[24]	—	T^2 [39]
ClO_4	6 kbar	Yes[25]	—	—
PF_6	ambient	—	T^2 [40]	$T^{1.8}$ [40], T^2 [41], $T^{1.5}$ [42]
PF_6	6 kbar	Yes[35]	—	—
PF_6	8-11 kbar	No[24,21,34]	T^2 [40,43], T [21]	$T^{1.8}$ [40]